Available online at www.sciencedirect.com

ScienceDirect

IFAC PapersOnline CONFERENCE PAPER ARCHIVE

IFAC PapersOnLine 55-22 (2022) 117–122

Experimental validation of an anti-windup design trading off position and heading direction control performance for quadrotor UAVs

Francesco Marzagalli * **Pietro Ghignoni** ** **Giovanni Gozzini** * **Davide Invernizzi** *

* *Dipartimento di Scienze e Tecnologie Aerospaziali, Politecnico di Milano, Via La Masa 34, 20156 Milano, Italy, (e-mail: francesco.marzagalli@mail.polimi.it, {giovanni.gozzini, davide.invernizzi}@polimi.it).*

** *Now Elecnor Deimos was with Politecnico di Milano during the development of this work, (e-mail: pietro.ghignoni@polimi.it).*

Abstract: We present the experimental validation of a recently developed anti-windup design to guarantee stability and a desired level of performance in the presence of propellers saturation in quadrotor UAVs. The considered solution exploits a decentralized LMI-based compensator to mitigate directionality issues affecting saturated multi-variable plants and to achieve satisfactory time-domain performance for reference signals of interest. After discussing saturation effects in quadrotors, we first show how the compensator can be implemented on top of a popular cascade control architecture for underactuated multi-rotors and then how it can be tuned to prioritize position/heading direction control objectives. The design is finally validated through experiments in representative flight conditions.

Keywords: Anti-windup, saturation, UAVs, position control, attitude control.

In recent years, quadrotor Unmanned Aerial Vehicles (UAVs) have attracted commercial and research interest for a variety of applications. While in most operating conditions linear control designs can be employed successfully, applications requiring high-performance tracking capabilities can overload the propulsive system and thus require a careful control design to deal with actuator saturation effects. Indeed, when using aggressive controllers, propellers are more likely to saturate, especially in complex maneuvers that involve combined position and yaw motions, due to an intrinsically inefficient yaw-torque generation mechanism.

Saturation effects in quadrotors are not only related to the well-known problem of integral windup but manifest also in the form of motions in undesired directions, a windup issue affecting saturated multi-variable plants. To briefly introduce the problem, we recall that classic control laws for quadrotors are based on a control allocation algorithm that mixes desired control thrust and torque using matrix inversion to compute the thrusts to be commanded to each propeller. When the commanded thrusts are saturated within a given range to respect the physical limitation of standard propellers for multi-rotors, which can deliver only a positive and bounded thrust, spurious torques appear along undesired axes, ultimately causing motions in unwanted directions. Windup directionality issues are commonly tackled in the literature about quadrotors by decoupling the control law that assigns the desired thrust and torque from the control allocation algorithm, which is solved in an optimal sense or by using iterative thrust-mixing schemes that prioritize roll-pitch control over thrust and yaw, see Smeur et al. (2017); Bezerra and Santos (2022); Faessler et al. (2017a); Brescianini and D'Andrea (2020). While Anti-Windup (AW) augmentation designs with formal stability and performance guarantees have been developed in recent years for directionality compensation, see Adegbege and Heath (2015); Biannic and Tarbouriech (2009), the application of these techniques to quadrotors case has been considered only in Ofodile and Turner (2016) and more recently in Ghignoni et al. (2021), which addressed the problem assuming a linear model.

In this paper, we show how the anti-windup augmentation design of Ghignoni et al. (2021) can be integrated within the nonlinear control architecture implemented in popular autopilots for quadrotors (*e.g.*, PX4 (2022)). Starting from the nonlinear model of a quadrotor UAV, we present the steps to obtain suitable linear closed-loop models needed for the anti-windup synthesis. The considered AW controller is a linear dynamic compensator with a decentralized structure which avoids by design the online solution of algebraic loops for a computationally efficient implementation on low cost hardware. Following Biannic and Tarbouriech (2009) and Ghignoni et al. (2021), the tuning of the compensator gains is cast as an LMI optimization problem, penalizing a weighted mismatch between the response of a suitably selected reference model and the response of the saturated system with AW compensation. By introducing a weight in the optimization procedure, the design allows synthesizing compensators capable of prioritizing control objectives, which is particularly useful in quadrotor applications wherein position control performance has typically higher priority over the heading direction one. Experimental results obtained in a maneuver that combines position and yaw reference setpoints confirm the capabilities of the proposed design in managing propeller saturation effects and in trading off the two different control objectives. A video of an experiment showing the benefit of the anti-windup augmentation also in off-design conditions can be watched at `https://youtu.be/GxyN35yfGKk`.

10.1016/j.ifacol.2023.03.020

Notation. In this paper $\mathbb{Z}(\mathbb{Z}_{>0}, \mathbb{Z}_{\geq 0})$ denotes the set of integers (positive, nonnegative integers), $\mathbb{R}(\mathbb{R}_{>0}, \mathbb{R}_{\geq 0})$ denotes the set of real numbers (positive, nonnegative real numbers). The ith vector of the canonical basis of $\mathbb{R}^n$ is denoted as e_i and the identity matrix in $\mathbb{R}^{n\times n}$ is denoted as $I_n := [e_1 \cdots e_i \cdots e_n]$. Given $A \in \mathbb{R}^{n\times n}$, we use the compact notation $A \in \mathbb{R}^{n\times n}_{>0}(\mathbb{R}^{n\times n}_{<0})$ to represent a positive (negative) definite matrix. For a square matrix X, we denote $\mathrm{He}(X) := X + X^\top$. Given a sequence $x(t), t \in \mathbb{Z}_{\geq 0}$, x^+ is a shorthand notation for $x(t+1)$. Function $\mathrm{sat}^{\bar{u}}_{\underline{u}}(\cdot)$ denotes the decentralized saturation function, *i.e.*, given $u \in \mathbb{R}^n$ and some bounds $\underline{u}, \bar{u} \in \mathbb{R}^n_{\geq 0}$, $\mathrm{sat}^{\bar{u}}_{\underline{u}}(u) := (\max(\min(\bar{u}_1, u_1), -\underline{u}_1), \ldots, \max(\min(\bar{u}_n, u_n), -\underline{u}_n))$. Finally, $\overline{\mathrm{co}}\{v_r \in \mathbb{R}^n,\ r = 1, \ldots, n_v\}$ is the closed convex hull, *i.e.*, the smallest closed convex set that contains the points identified by the vectors v_r. The set $\mathrm{SO}(3) := \{R \in \mathbb{R}^{3\times 3} : R^\top R = I_3, \det(R) = 1\}$ denotes the three-dimensional Special Orthogonal group. The map $S(\cdot) : \mathbb{R}^3 \to \mathfrak{so}(3) := \{W \in \mathbb{R}^{3\times 3} : W = -W^\top\}$ is defined such that given $a, b \in \mathbb{R}^3$ one has $S(a)b = a \times b$. The inverse of the S map is denoted with $S^{-1} : \mathfrak{so}(3) \mapsto \mathbb{R}^3$.

1. MODELING AND BASELINE CONTROL DESIGN FOR QUADROTOR UAVS

We start by showing the dynamical model of quadrotor UAVs commonly employed for control design purposes, and then we present a baseline cascade control architecture, similar to the one implemented in popular autopilots, to stabilize the quadrotor position and heading direction.

1.1 Mathematical model

A quadrotor UAV is an aerial vehicle made by a central body and *4* arms, each of which carries a propeller. The configuration of the rigid UAVs can be identified with the motion of a body-fixed frame $F_B := (O_B, \{b_1, b_2, b_3\})$ with respect to a reference frame $F_I := (O_I, \{i_1, i_2, i_3\})$, where b_j and i_j for $j \in \{1, 2, 3\}$ are unit vectors forming right-handed orthogonal triads and O_B, O_I are the origins of the body and reference frame, respectively. In the following, the position vector from O_I to O_B, resolved in F_I, is denoted as $x \in \mathbb{R}^3$ while the rotation matrix describing the attitude of the UAV is denoted as $R := [b_1\ b_2\ b_3] \in \mathrm{SO}(3)$, where b_i is the *i-th* body axis resolved in F_I. The dynamical model of a vectored-thrust UAV can be described by

$$\dot{R} = RS(\omega) \qquad J\dot{\omega} = -S(\omega)J\omega + \tau_e + \tau_c \tag{1}$$

$$\dot{x} = v \qquad m\dot{v} = -mge_3 + T_c Re_3 + f_e, \tag{2}$$

where $J = J^\top \in \mathbb{R}^{3\times 3}_{>0}$ is the UAV inertia matrix with respect to O_B, $m \in \mathbb{R}_{>0}$ is UAV mass, $g = 9.81\,\mathrm{m/s^2}$ is the gravitational acceleration, $\omega \in \mathbb{R}^3$ is the body angular velocity, $v \in \mathbb{R}^3$ is the inertial translational velocity, $T_c > 0$ and $\tau_c \in \mathbb{R}^3$ are the overall thrust and the torque applied by the propellers, respectively, and $(f_e, \tau_e) \in \mathbb{R}^6$ is the disturbance wrench. Following a consolidated approach in the literature about small-scale quadrotors of Brescianini and D'Andrea (2020), T_c and τ_c are related to the individual thrusts delivered by the propellers (T_1, T_2, T_3, T_4) through the linear map

$$\begin{bmatrix} T_c \\ \tau_{c_1} \\ \tau_{c_2} \\ \tau_{c_3} \end{bmatrix} = \underbrace{\begin{bmatrix} 1 & 1 & 1 & 1 \\ \ell\sin(\beta_1) & \ell\sin(\beta_2) & \ell\sin(\beta_3) & \ell\sin(\beta_4) \\ -\ell\cos(\beta_1) & -\ell\cos(\beta_2) & -\ell\cos(\beta_3) & -\ell\cos(\beta_4) \\ \sigma & -\sigma & \sigma & -\sigma \end{bmatrix}}_{X} \begin{bmatrix} T_1 \\ T_2 \\ T_3 \\ T_4 \end{bmatrix}, \tag{3}$$

where $X \in \mathbb{R}^{4\times 4}$ is the control effectiveness matrix, $\ell > 0$ is the distance from the *i-th* rotor hub to O_B, $\sigma > 0$ is the ratio between the propeller thrust and torque coefficient and $\beta_i = \pi/4 + \pi/2(i-1)$ (cross-configuration) is the angle about the b_3 axis between each pair of axes of the arms.

1.2 Cascade control design for position-yaw stabilization

Given that X is invertible, assuming no bounds on the propeller thrusts, it possible to apply the preliminary feedback

$$\begin{bmatrix} T_1\ T_2\ T_3\ T_4 \end{bmatrix}^\top = X^{-1} \begin{bmatrix} T_c^d\ \tau_c^{d\top} \end{bmatrix}^\top \tag{4}$$

to (3) and use $T_c^d > 0$ and $\tau_c^d \in \mathbb{R}^3$ as variables for control design purposes, representing a desired control thrust and torque, respectively. By relying on the differential flatness property of the dynamics (1)-(2) with respect to the position vector x and to the rotation about the b_3 axis, see Invernizzi et al. (2018), several control strategies have been proposed in the literature to deal with the nonlinear and underactuated nature of the quadrotor dynamics. In this work we consider a nonlinear cascaded controller for position-yaw setpoint regulation, with the same structure of the one implemented in the PX4 autopilot PX4 (2022). Specifically, the control architecture corresponds to a double cascade of P/PID nonlinear controllers for position and attitude control with a planner in the middle (see Figure 1):

$$f_c^d := PI_x(z)(k^o_{p,x}(x - x^d) - v) - D_x(z)v + mge_3 \tag{5}$$

$$\begin{cases} T_c^d := \|f_c^d\| \\ R_p := \left[\frac{b_{p_3}\times b_{d_1}}{\|b_{p_3}\times b_{d_1}\|} \times b_{p_3} \quad \frac{b_{p_3}\times b_{d_1}}{\|b_{p_3}\times b_{d_1}\|} \quad b_{p_3} \right], b_{p_3} := \frac{f_c^d}{\|f_c^d\|} \end{cases} \tag{6}$$

$$\tau_c^d := PI_R(z)\left(\omega^d(K_{p,R}(R_p^\top R)) - \omega\right) - D_R(z)\omega, \tag{7}$$

where $PI_{(\cdot)}(z) := k^i_{p,(\cdot)} + k^i_{i,(\cdot)} t_s \frac{1}{z-1}$, $D_{(\cdot)}(z) := k^i_{d,(\cdot)} N^i_{(\cdot)} \frac{z-1}{z-1+N^i_{(\cdot)} t_s}$ are discrete transfer functions defining, respectively, a proportional integral and (filtered) derivative actions, $t_s \in \mathbb{R}_{>0}$ denotes the sampling time, $k^{(\cdot)}_{(\cdot,\cdot)} \in \mathbb{R}_{>0}$ are scalar gains while $K_{p,R} \in \mathbb{R}^{3\times 3}_{>0}$ is a diagonal gain matrix and $N^{(i)}_{(\cdot)} \in \mathbb{R}_{>0}$ is the filter time constant; $x^d \in \mathbb{R}^3$ is the position setpoint; the rotation matrix $R_p \in \mathrm{SO}(3)$ is the reference signal to be tracked by the attitude controller (7) and corresponds to a reference frame having the third axis b_{p_3} aligned with the force required for position stabilization (f_c^d in (5)) while the other two axes of the frame are assigned by a rotation about b_{p_3} that accounts for a desired yaw angle ($\psi^d \in \mathbb{R}$) through the unit vector $b_{d_1} := [\cos(\psi^d)\ \sin(\psi^d)\ 0]^\top$, which represents the desired (inertial) heading direction; $\omega^d(K_{p,R}R_p^\top R) := 2K_{p,R}\mathrm{sgn}(\mathrm{q}_e(R_p))\mathbf{q}_e(R_p)$ is a nonlinear proportional stabilizer assigning the reference velocity to the inner-loop attitude PID controller, with $\mathrm{q}_e(R_p) \in \mathbb{R}$ and $\mathbf{q}_e(R_p) \in \mathbb{R}$ being the vectorial and the scalar part of the quaternion error $q_e \in \mathbb{S}^3$, respectively (see (PX4, 2022, Multicopter Attitude Controller) for additional details).

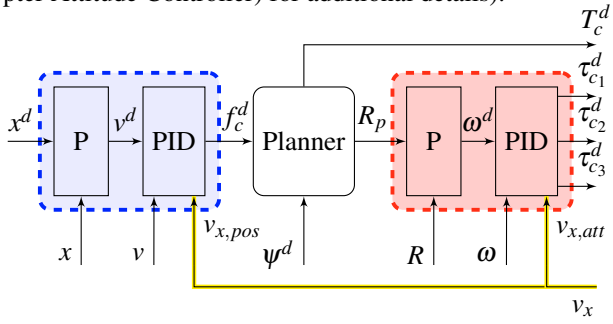

Fig. 1. Baseline controller implementation.

2. SATURATION EFFECTS IN QUADROTORS

Common propellers for quadrotors are unidirectional and have finite power, meaning that they can deliver only a positive and bounded thrust along their spinning axis, *i.e.*, $0 \leq T_i \leq T_M$ $\forall i \in \{1,\dots,4\}$. Saturation effects are sometimes accounted for in the literature, Invernizzi et al. (2018); Cao and Lynch (2016), by designing control laws that guarantee T_c^d, τ_c^d be bounded. While reasonable, such an approach does not guarantee that the physical inputs T_i, computed by inverting the input map as in (4), are feasible, namely, positive and upper bounded by T_M. When saturation occurs, one cannot transfer the commanded action T_c^d, τ_c^d to the quadrotor and the actual allocation $X\text{sat}\left(X^{-1}\left[T_c^d \ \tau_c^{d\top}\right]^\top\right)$ induces cross coupling phenomena among the different inputs, giving rise to undesirable effects known as *directionality* issues in the literature on saturated multivariable plants.

The reason why the baseline controller (5)-(7) is often used in practice without accounting for saturation effects is that saturation bounds are hardly hit in standard operating conditions: quadrotors are designed to hover about 50% of the available thrust, giving them more than enough margin to allocate control actions for standard maneuvers. Nonetheless, when looking for high performance controllers, abrupt maneuvers (*e.g.*, step references or large initial errors with respect to the desired trajectory) or operations in off-design conditions (*e.g.*, heavy payload transportation, wind disturbances) can make the propellers saturate and therefore induce windup effects which are mainly associated with the induced cross-coupling among the inputs. Moreover, trajectories combining position and yaw motions are prone to actuators saturation due to the lower effectiveness of the yaw-torque generation mechanism with respect to the roll-pitch one (the coefficient σ in (3) has a small value compared to the arm length ℓ). One way to address this issue is to reduce the aggressiveness of yaw control or to scale down the commanded yaw torque τ_{c_3} until saturations are not reached any more when inverting (3) (at least until possible, see Faessler et al. (2017b); Brescianini and D'Andrea (2020)). In contrast, the approach that we propose here is based on a systematic design of an AW augmentation scheme which allows one to prioritize control objectives.

3. DECENTRALIZED ANTI-WINDUP AUGMENTATION STRATEGY FOR INPUT-COUPLED PLANTS

In this Section we recall the decentralized AW design proposed in Ghignoni et al. (2021), which is cast as an LMI-based optimization problem following the modern framework of the Direct Linear Anti-Windup (DLAW) design in Galeani et al. (2009) and leveraging the performance-oriented approach presented in Biannic and Tarbouriech (2009).

3.1 Performance-oriented AW design

To implement the proposed AW strategy, the quadrotor model in (8)-(9) must be linearized. Assuming near hovering conditions at a given position $\bar{x} \in \mathbb{R}^3$, *i.e.*, $x \approx \bar{x} + \Delta x$, $v \approx \Delta v$, $R \approx I_3 + S(\Delta\alpha)$ with $\Delta\alpha := \left[\phi \ \theta \ \psi\right]^\top$ being small rotation angles, $\omega \approx \Delta\omega$, the linearized quadrotor dynamics reads:

$$\dot{\Delta\alpha} = \Delta\omega, \qquad \dot{\Delta x} = \Delta v \tag{8}$$

$$J\dot{\Delta\omega} = \Delta\tau_c, \qquad m\dot{\Delta v} = mgS(\Delta\alpha)e_3 + \Delta T_c e_3, \tag{9}$$

in which $\Delta T_c := T_c - mg$ and $\Delta\tau_c := \tau_c$ and $\Delta(\cdot)$ represent deviation variables. Such a model can be cast in the form of a linearized discrete time-invariant plant

$$(P) \quad \begin{cases} x_p^+ = A_p x_p + B_{p,u} u \\ y = C_{p,y} x_p + D_{p,yu} u \\ z = C_{p,z} x_p + D_{p,zu} u, \end{cases} \tag{10}$$

where the state space matrices have a block-diagonal structure with 4 blocks, $x_p \in \mathbb{R}^{n_p}$ is the state vector, the plant output is $y := \left[\Delta x^\top \ \Delta\alpha^\top \ \Delta v^\top \ \Delta\omega^\top\right]^\top \in \mathbb{R}^{12}$, the performance output is $z := \left[x^\top \ \psi\right]^\top \in \mathbb{R}^4$ and $u := \left[\Delta T_c \ \Delta\tau_c^\top\right]^\top \in \mathbb{R}^4$ is the input vector. The linearized closed-loop system (8)-(9) has a block-diagonal structure made by four subsystems: the altitude (x_3), the longitudinal-lateral (x_2,ϕ)-(x_1,θ) and the yaw (ψ) subsystems, respectively controlled by ΔT_c, $\Delta\tau_{c_1}$, $\Delta\tau_{c_2}$ and $\Delta\tau_{c_3}$. According to (4), input u is a mixing of the actual plant inputs $u_a = \left[\Delta T_1 \ \Delta T_2 \ \Delta T_3 \ \Delta T_4\right]^\top \in \mathbb{R}^4$, where $\Delta T_i = T_i - \frac{mg}{4}$ $\forall i \in \{1,2,3,4\}$, through the (non-singular) matrix $X \in \mathbb{R}^{4\times 4}$, *i.e.*, $u = Xu_a$.

Similarly, the control law can be linearized by recognizing that $\omega^d(K_{p,R}R_p^\top R) \approx K_{p,R}\left[\phi-\phi_p \ \theta-\theta_p \ \psi-\psi^d\right]^\top$ and $\|f_c^d\| \approx mg$ in near hovering conditions, so as to obtain:

$$\Delta T_c^d := PI_{x_3}(z)\left(k_{p,x_3}^o(x_3^d - x_3) - v_3\right) - D_{x_3}(z)v_3 \tag{11}$$

$$\Delta\tau_c^d := PI_R(z)\left(K_{p,R}\left[\phi_p-\phi \ \theta_p-\theta \ \psi^d-\psi\right]^\top - \omega\right) - D_R(z)\omega, \tag{12}$$

where the virtual roll and pitch angles are

$$\phi_p := \tfrac{1}{mg}\left(PI_{x_2}(z)\left(k_{p,x_2}^o(x_2^d - x_2) - v_2\right) - D_{x_2}(z)v_2\right), \tag{13}$$

$$\theta_p := -\tfrac{1}{mg}\left(PI_{x_1}(z)\left(k_{p,x_1}^o(x_1^d - x_1) - v_1\right) - D_{x_1}(z)v_1\right) \tag{14}$$

while ψ_d is the desired yaw angle. The linearized control law can be compactly written as

$$(C) \quad \begin{cases} x_c^+ = A_c x_c + B_{c,y} y + B_{c,w} w + v_x \\ y_c = C_c x_c + D_{c,y} y + D_{c,w} w + v_y, \end{cases} \tag{15}$$

where again the state space matrices are made of 4 subsystems, $x_c \in \mathbb{R}^{n_c}$ $(n_c = 2\cdot 6)$ is the state of the controller, $y_c = \left[\Delta T_c^d \ \Delta\tau_c^{d\top}\right]^\top \in \mathbb{R}^{n_{y_c}}$ $(n_{y_c} = 4)$ is the corresponding output, $w := \left[x^{d\top} \ \psi^d\right]^\top \in \mathbb{R}^4$ is the set-point and $v_x \in \mathbb{R}^{n_c}$, $v_y \in \mathbb{R}^{n_{c_y}}$ are additional inputs to be used for the AW augmentation. When assuming no bound for u_a, by exploiting the invertibility of X, the interconnection of (P) and (C) through the allocation $u_a = X^{-1}y_c$ yields four decoupled subsystems which are assumed to be well posed and internally stable.

In practice, due to actuator saturation, each u_{a_i} is bounded between $[-\underline{u}_i, \bar{u}_i]$, and the interconnection of (P) and (C) by

$$u_a = \text{sat}_{\underline{u}}^{\bar{u}}(X^{-1}y_c), \tag{16}$$

forms the *constrained* closed-loop system. Whenever X is not diagonal, the closed loop loses its decentralized structure during saturation. The compensation signals v_x, v_y injected into (15) are computed as outputs of the linear filter

$$(AW) \quad \begin{cases} x_{aw}^+ = B_{aw} q_X \\ \begin{bmatrix} v_x \\ v_y \end{bmatrix} = \begin{bmatrix} 0 \\ I_{n_u} \end{bmatrix} x_{aw} + \underbrace{\begin{bmatrix} \bar{D}_{aw} \\ 0_{n_u} \end{bmatrix}}_{D_{aw}} q_X, \end{cases} \tag{17}$$

$$q_X := y_c - X\text{sat}_{\underline{u}}^{\bar{u}}(X^{-1}y_c) \tag{18}$$

where $x_{aw} \in \mathbb{R}^{n_{y_c}}$ is the state of the AW filter while $B_{aw} \in \mathbb{R}^{n_{y_c}\times n_{y_c}}$ and $\bar{D}_{aw} \in \mathbb{R}^{n_c \times n_{c_y}}$ are tunable matrices. The proposed

AW filter corresponds to a static full-authority AW compensator in which the signal v_y is cascaded with a unit delay in order to avoid solving in real time implementations the algebraic loop arising in the controller.

The interconnection of (10), (15) and (17) through q_X can be written in compact form by introducing the *augmented* closed-loop (ACL):

$$(ACL) \quad \begin{cases} x_a^+ = A_a x_a + B_{a,q} q_X + B_{a,w} w \\ z = C_{a,z} x_a + D_{a,zq} q_X + D_{a,zw} w \\ y_c = C_{a,u} x_a + D_{a,uq} q_X + D_{a,uw} w, \end{cases} \tag{19}$$

where $x_a := (x_p, x_c, x_{aw})$. Following the performance-oriented AW design of Biannic and Tarbouriech (2009), we consider the reference model (RM)

$$(RM) \quad \begin{cases} x_{rm}^+ = A_{rm} x_{rm} + B_{rm,w} w \\ z_{rm} = C_{rm,z} x_{rm} + D_{rm,zw} w \end{cases} \tag{20}$$

to describe the desired unconstrained closed-loop behavior. As conditions inducing propeller saturation can be assimilated with the use of step references, we include the filter

$$(F) \quad w^+ = I_{n_w}(1-\varepsilon)w, \quad w(0) = w_0, \quad 0 < \varepsilon \ll 1, \tag{21}$$

into the closed-loop system used for the AW synthesis, as suggested in Biannic and Tarbouriech (2009) to achieve good time-domain responses in practical conditions (the initial condition of the filter w_0 can be considered as the step amplitude). Thus, by defining the augmented state $\xi = (x_a, x_{rm}, w) \in \mathbb{R}^{n_\xi}$, the interconnection of (19), (20) and (21) through q_X is given compactly by

$$\begin{cases} \xi^+ = A\xi + B_q q_X \\ z_e = C_z \xi + D_{zq} q_X \\ y_c = C_y \xi + D_{yq} q_X, \end{cases} \tag{22}$$

where all the involved matrices can be uniquely determined from (10), (15), (17), (20) and (21) and where

$$z_e := z - z_{rm} \tag{23}$$

is a performance output introduced to evaluate the mismatch between the reference and the actual system response.

3.2 Fixed-dynamics AW compensator synthesis

We now report for completeness the AW synthesis result presented in Ghignoni et al. (2021).

Theorem 1. Consider the augmented system in (22), define n_r directions of interest $r_1, \dots, r_{n_r} \in \mathbb{R}^{n_w}$ and select a diagonal matrix $W \in \mathbb{R}^{n_z \times n_z}_{\geq 0}$ to be used for control objectives prioritization. If there exist matrices $Q = Q^\top \in \mathbb{R}^{n_\xi \times n_\xi}_{>0}$, $Y \in \mathbb{R}^{n_{cy} \times n_\xi}$, $U \in \mathbb{R}^{n_{cy} \times n_{cy}}_{>0}$ diagonal, $\hat{B}_{aw} \in \mathbb{R}^{n_{yc} \times n_{yc}}$, $\hat{D}_{aw} \in \mathbb{R}^{(n_c + n_{yc}) \times n_{yc}}$ and a scalar $\gamma \in \mathbb{R}_{>0}$ satisfying

$$\mathrm{He} \begin{bmatrix} -\frac{Q}{2} & QC_y^\top & 0 & 0 \\ -XY & -G + D_{cl,uq}G + D_{cl,uv}\hat{D}_{aw} & 0 & 0 \\ WC_zQ & W\left(D_{cl,zq}G + D_{cl,zv}\hat{D}_{aw}\right) & -\frac{\gamma}{2} I_{n_z} & 0 \\ AQ & \begin{bmatrix} B_{cl,q}G + B_{cl,v}\hat{D}_{aw} \\ \hat{B}_{aw} \\ 0 \end{bmatrix} & 0 & -\frac{Q}{2} \end{bmatrix} < 0,$$

$$\begin{bmatrix} \bar{\bar{u}}_i^2 & Y_i \\ Y_i^\top & Q \end{bmatrix} \geq 0, \quad \hat{D}_{aw_{jk}} = 0, \quad \begin{bmatrix} Q & \begin{bmatrix} 0 \\ r_h \end{bmatrix} \\ \begin{bmatrix} 0 & r_h^\top \end{bmatrix} & 1 \end{bmatrix} \geq 0, \tag{24}$$

where $G := XUX^\top$, Y_i denotes the *i-th* row of Y ($i = 1, \dots, n$), $\bar{\bar{u}}_i := \min(\underline{u}_i, \bar{u}_i)$ is the *i-th* input bound, $B_{cl,q}$, $B_{cl,v}$, $D_{cl,uq}$, $D_{cl,uv}$, $D_{cl,zq}$, $D_{cl,zv}$ are defined as in Appendix A, $\hat{D}_{aw_{jk}}$ is the element in the *j-th* row *k-th* column of $\hat{D}_{aw}$ ($j \in \{n_c + 1, \dots, n_c + n_{y_c}\}$, $k \in \{1, \dots n_c\}$) and $h \in \{1, \dots n_r\}$, then by selecting the anti-windup matrices in (17) as

$$B_{aw} = \hat{B}_{aw} G^{-1} \tag{25}$$

$$D_{aw} = \hat{D}_{aw} G^{-1}, \tag{26}$$

the ellipsoid $\mathscr{E}(Q^{-1}) := \left\{\xi \in \mathbb{R}^{n_\xi} : \xi^\top Q^{-1} \xi \leq 1\right\}$ is contained in the region of attraction of (22) and the closed convex hull $\overline{\mathrm{co}}\{(0, r_h) \in \mathbb{R}^{n_\xi}, h = 1, \dots, n_r\} \subset \mathscr{E}(Q^{-1})$. Moreover, the following condition on the ℓ_2 norm of z_e is satisfied:

$$\sum_{t=0}^{\infty} z_e^\top W^2 z_e \leq \gamma, \quad \forall \xi(0) \in \mathscr{E}(Q^{-1}). \tag{27}$$

Since the smaller γ, the lower the mismatch z_e weighted by W, the tuning of the AW compensator can be cast as the solution of the following semidefinite program:

$$\min_{Q, Y, U, \gamma, \hat{B}_{aw}, \hat{D}_{aw}} \gamma, \quad \text{subject to (24).} \tag{28}$$

The matrices of the optimal anti-windup controller can then be recovered using (25) and (26).

The proposed synthesis method is based on the selection of suitable step amplitudes, through the choice of the vectors r_i, and on the definition of a suitable weight matrix W. While the selection of the former is guided by the operating environment of the drone, the selection of W allows the control designer to penalize selectively the components of z_e and therefore to trade-off different tracking performance objectives. As z_e is a vector that collects the error between the position coordinates and the yaw angle with respect to corresponding quantities generated by the reference model, an effective choice to achieve a desired behavior is to use a diagonal W having null elements for the output component(s) with the least priority. A few such choices will be shown in the experimental results described in the next section.

4. EXPERIMENTAL RESULTS

This section reports flight test results obtained using a quadrotor UAV developed by ANT-X, a spin-off company of Politecnico di Milano. The experiments have been performed in the Flying Arena for Rotorcraft Technologies (FlyART) at Politecnico di Milano, an indoor facility equipped with a Motion Capture (Mo-Cap) and a ground control station to send the desired trajectory and the measurements (position and attitude) from the Mo-Cap system to the quadrotor computer. The baseline controller (5)-(7) has been augmented by the AW compensator in (17): the signal v_y is injected to the desired inputs T_c^d, τ_c^d, while v_x is used to compensate the states of the controller. As shown in Figure 1, the highlighted signal v_x is partitioned in two contributions: $v_{x,pos}$, which affects the north, east, down velocity PID state equation, and $v_{x,att}$, which modifies the roll, pitch, yaw rate PID state equation. The augmented controller has been developed in Simulink and then integrated within the PX4 autopilot using the ANT-X rapid prototyping system.

To show how directionality windup issues can affect the performance of quadrotors, we have considered an aggressive maneuver made of step references which combine lateral-vertical and yaw motions characterized by quite large amplitudes ($x_1^d(t) := 0\text{m}$, $x_2^d(t) := 4\,\text{step(t} - 1)\text{m}$, $x_3^d(t) := 2\,\text{step(t} - 1)\text{m}$ and $\psi^d(t) := 30\,\text{step(t} - 1)\,\text{deg}$). The tuning procedure

presented in Section 3.2 has been carried out by exploiting identified linear discrete-time models of the dynamics of the ANT-X drone. The solution to the optimization problem in (28) has then been obtained by referring to the convex set contained in the polyhedron made by eight vertices r_i. $i \in \{1,2,\ldots,8\}$ corresponding to combinations of $(\pm 4\text{m}, 0\text{m}, 2\text{m}, \pm\pi/6\text{rad})$ and $(0\text{m}, \pm 4\text{m}, 2\text{m}, \pm\pi/6\text{rad})$. As in Ghignoni et al. (2021), the resulting AW compensator (17) is decentralized for the considered vertices r_i, *i.e.*, the compensator has a block-diagonal structure without cross-couplings terms that would themselves induce some directionality effects (see (Ghignoni et al., 2021, Remark 2) and Ofodile and Turner (2016) for a thorough discussion on this aspect).

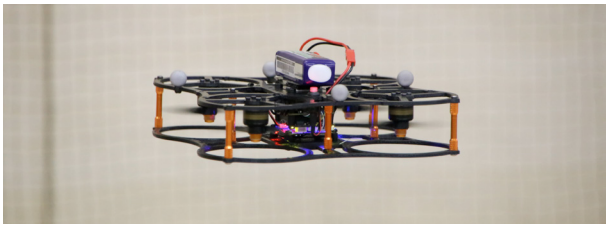

Fig. 2. The ANT-X quadrotor.

The experiments have been conducted by considering three different tuning sets of the AW compensator in (17), corresponding to a different level of priority between position and heading performance objectives, which can be imposed at synthesis time by properly selecting matrix W. The first tuning set corresponds to high position priority, which is obtained by setting $W = \text{diag}(1,1,1,0)$ in (24). The effect of saturation in the form of directionality windup can be appreciated in Figure 3, where the setpoint tracking results are presented. The red-dashed line shows the degraded performance of the baseline controller: propellers saturation triggers an undesired oscillating response along the x_1 axis (for which the setpoint is zero) with a maximum peak of more than 20 cm. The effectiveness of the proposed AW compensator (green-continuous line) is noticeable: directionality effects almost disappear (top plot) and by inspecting the step response along the x_2 direction (second plot), the compensated response is faster and has a smaller overshoot with respect to the saturated case (11% vs 19%). As for the assessment of yaw tracking performance, the bottom plot in Figure 3 shows that the AW controller (green-continuous line) has a worse performance than the saturated controller (red-dashed line). This is not a surprising result since the weight W on the mismatch between the desired yaw angle and the actual one has set to zero during the AW synthesis in order to give full priority to position control.

To appreciate the effect of control objective prioritization, the selection $W = \text{diag}(0,0,1,1)$ was also consider to favor altitude and yaw tracking performance over longitudinal and lateral position tracking. By inspecting Figure 4, it is clear that by weighting more the yaw error one achieves a much more desirable response to heading direction setpoint: the blue-dashed-dotted line in the bottom pane reports no overshoot and a faster response with respect to the saturated controller and to the AW compensator designed for position priority $(W = \text{diag}(1,1,1,0))$. As expected, since no weight was placed on the tracking error along x_1 direction, a less desirable response is obtained with a larger overshoot along the x_1 axis (top plot). Figure 5 illustrates the case in which the compensator was synthesized by equally prioritizing all the objectives $(W = \text{diag}(1,1,1,1))$: while directionality issues are not fully compensated (top plot, magenta-dashed line), the yaw tracking performance is remarkably better than the case of full position priority (bottom plot, magenta-dashed vs green continuous line). Finally, an off design condition has been tested by assigning a large yaw setpoint $(\psi_d(t) = 150\text{step}(t-1)\,\text{deg})$. The aggressiveness of the considered maneuver can be seen in Figure 6, where the time histories of the normalized thrusts commanded to the propellers are reported. Looking at Figure 7, the response of the AW controller with position priority (green-continuous line) shows a marked improvement with respect to the saturated response (red-dashed line), which is characterized by a very large lateral motion.

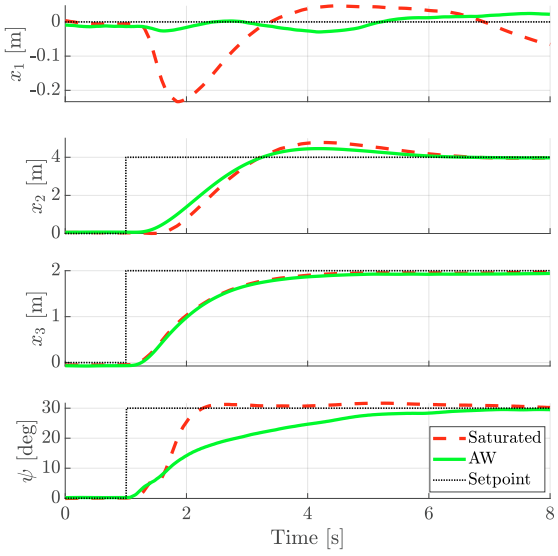

Fig. 3. Quadrotor position and heading time history.

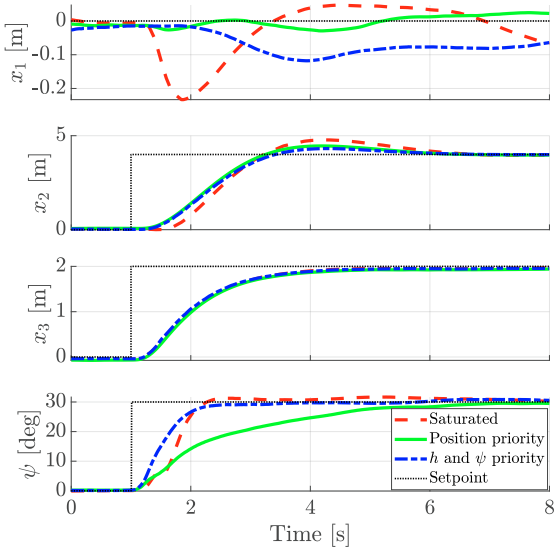

Fig. 4. Tracking performance with weighted yaw.

5. CONCLUSION

This paper has dealt with the problem of windup and directionality effects that arise in small quadrotors. A nonlinear baseline controller, similar to the one implemented in popular autopilots, has been augmented with a decentralized, performance-oriented, AW compensator. Following Ghignoni et al. (2021), the compensator was synthesized according to the DLAW

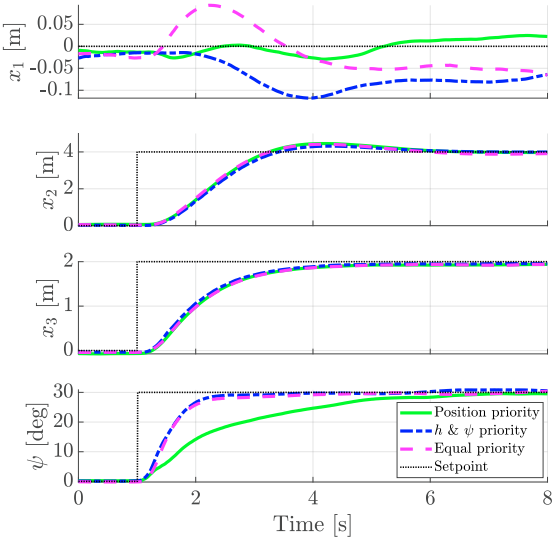

Fig. 5. Three different priority levels tracking performance comparison.

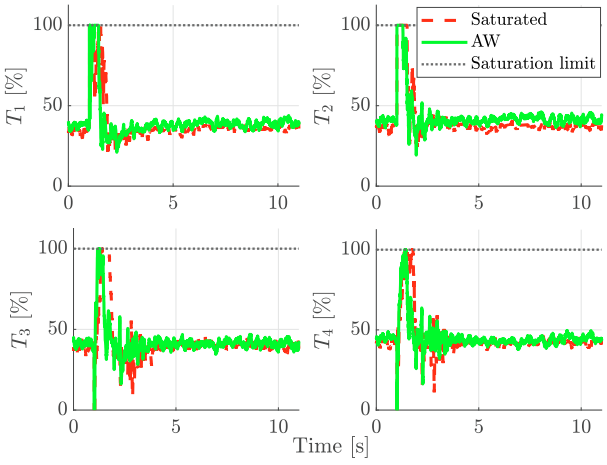

Fig. 6. Quadrotor inputs time history.

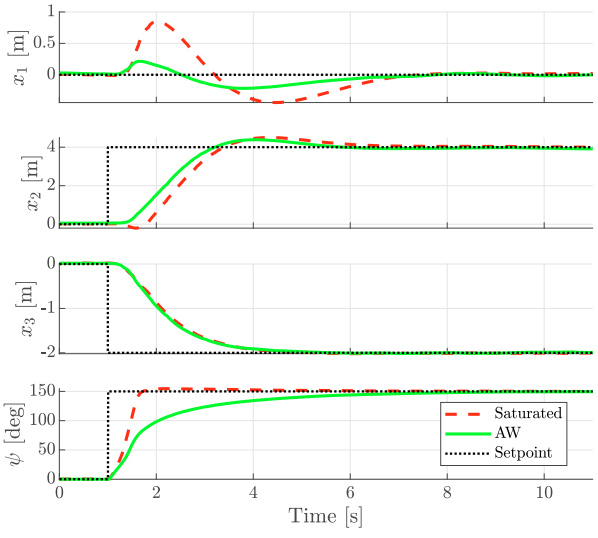

Fig. 7. Quadrotor position and heading time history.

framework through an LMI-based method, and by introducing a suitable weight that allows to trade-off position and heading direction control performance. The augmented design has been tested through flight experiments which confirmed the effectiveness of the proposed scheme to solve the problems induced by the saturation of the propellers.

REFERENCES

Adegbege, A.A. and Heath, W.P. (2015). Directionality compensation for linear multivariable anti-windup synthesis. *International Journal of Control*, 88(11), 2392–2402.

Bezerra, J.A. and Santos, D.A. (2022). Optimal exact control allocation for under-actuated multirotor aerial vehicles. *IEEE Control Systems Letters*, 6, 1448–1453.

Biannic, J.M. and Tarbouriech, S. (2009). Optimization and implementation of dynamic anti-windup compensators with multiple saturations in flight control systems. *Control Engineering Practice*, 17(6), 703 – 713.

Brescianini, D. and D'Andrea, R. (2020). Tilt-prioritized quadrocopter attitude control. *IEEE Transactions on Control Systems Technology*, 28(2), 376–387.

Cao, N. and Lynch, A. (2016). Inner–Outer Loop Control for Quadrotor UAVs With Input and State Constraints. *IEEE Transactions on Control Systems Technology*, 24(5), 1797 – 1804.

Faessler, M., Falanga, D., and Scaramuzza, D. (2017a). Thrust mixing, saturation, and body-rate control for accurate aggressive quadrotor flight. *IEEE Robotics and Automation Letters*, 2(2), 476–482.

Faessler, M., Falanga, D., and Scaramuzza, D. (2017b). Thrust mixing, saturation, and body-rate control for accurate aggressive quadrotor flight. *IEEE Robotics and Automation Letters*, 2(2), 476–482.

Galeani, S., Tarbouriech, S., Turner, M., and Zaccarian, L. (2009). A tutorial on modern anti-windup design. *European Journal of Control*, 15(3), 418 – 440.

Ghignoni, P., Buratti, N., Invernizzi, D., and Lovera, M. (2021). Anti-windup design for directionality compensation with application to quadrotor UAVs. *IEEE Control Systems Letters*, 5(1), 331–336.

Invernizzi, D., Lovera, M., and Zaccarian, L. (2018). Geometric tracking control of underactuated VTOL UAVs. In *American Control Conference*. Milwaukee (WI), USA.

Ofodile, N. and Turner, M. (2016). Decentralized approaches to antiwindup design with application to quadrotor unmanned aerial vehicles. *IEEE Transactions on Control Systems Technology*, 24(6), 1980 – 1992.

PX4 (2022). PX4 autopilot user guide, last access: July 2022. `https://docs.px4.io/v1.12/en/flight_stack/controller_diagrams.html`.

Smeur, E., Höppener, D., and De Wagter, C. (2017). Prioritized control allocation for quadrotors subject to saturation. In *Int. Micro MAV Conference and Flight Competition*, 37–43.

Appendix A. EXPRESSIONS OF THE MATRICES APPEARING IN LMI (24)

Given $\Delta_u := (I_n - D_{c,y}D_{p,yu})^{-1}$, $\Delta_y := \left(I_{n_y} - D_{p,yu}D_{c,y}\right)^{-1}$ the matrices to be defined in LMI (24) are:

$$\left[\begin{array}{c} B_{cl,q} \\ \hline D_{cl,zq} \\ D_{cl,uq} \end{array}\right] := \left[\begin{array}{c} -B_{p,u}\Delta_u \\ \hline -B_{c,y}\Delta_y D_{p,yu} \\ -D_{p,zu}\Delta_u \\ \hline I_n - \Delta_u \end{array}\right], \quad \left[\begin{array}{c|c} B_{cl,y} & \\ \hline D_{cl,uv} & \\ D_{cl,zv} & \end{array}\right] := \left[\begin{array}{cc} 0 & B_{p,u}\Delta_u \\ I_{n_c} & B_{c,y}\Delta_y D_{p,yu} \\ \hline 0 & \Delta_u \\ 0 & D_{p,zu}\Delta_u \end{array}\right]. \quad \text{(A.1)}$$